ChemComm

COMMUNICATION

View Article Online
View Journal | View Issue

Cite this: *Chem. Commun.*, 2021, **57**, 7180

Received 28th May 2021,
Accepted 24th June 2021

DOI: 10.1039/d1cc02805g

rsc.li/chemcomm

Evolution of catalytic machinery: three-component nanorotor catalyzes formation of four-component catalytic machinery†

Abir Goswami,‡ Merve S. Özer,‡ Indrajit Paul and Michael Schmittel *

The three-component nanorotor $[Cu_2(S)(R)]^{2+}$ (k_{298} = 46.0 kHz) that is a catalyst for a CuAAC reaction binds the click product at each of its copper centers thereby creating a new platform and a dynamic slider-on-deck system. Due to this sliding motion (k_{298} = 65.0 kHz) the zinc-porphyrin bound *N*-methylpyrrolidine is efficiently released into solution and catalyzes a follow-up Michael addition.

For many chemists, the unmatched performance of Nature's multicomponent machinery has been an inspiration for developing supramolecular machines that exhibit mechanical motion and perform useful tasks.[1] However, one aspect of Nature's road to machinery has received little attention so far: new enzymes with alternative architectures and new functions are constantly being evolved from their ancestral enzymes.[2,3] Evolution of new artificial machinery from a dynamic information–handling mixture[4] or directly from multicomponent machines[5] is thus a persuasive vision. However, despite remarkable developments in the field of useful molecular machines,[6] only an outstanding paper by Leigh reports on a manmade machine building another functional device, in this case, a homooligomeric peptide for asymmetric catalysis.[7]

Knowledge of adaptive dynamic supramolecular devices[8] is continuously growing and will eventually help to approach the complexity and seamless organization of biological systems.[9] Recently, we have reported catalytic multicomponent machinery[10] like rotors, walker, and sliders based on heteroleptic metal–ligand complexation and demonstrated how emergent functionality evolved from well-conceived self-sorting.[11] Yet, transformation of a manmade machine to new dynamic catalytic machinery remains without precedent. Here, we demonstrate how the three-component nanorotor $[Cu_2(S)(R)]^{2+}$ (**S** = stator; **R** = rotator/slider) *via* CuAAC chemistry catalyzes formation of the four-component slider-on-deck $[Cu_2(S)(R)(P)_2]^{2+}$ (Scheme 1), where the latter acts as catalytic machinery turning ON a Michael addition reaction.

The design of this unique transformation is based on the nanorotor $[Cu_2(S)(R)]^{2+}$ (Scheme 1) whose catalytic activity for azide–alkyne cycloadditions has been established.[10a] In that work, we demonstrated that the click product was expelled from the catalytic site by the nanomechanical motion in the nanorotor.[12] For the present project, we chose the reactants **1** and **2** in such a way that their bidentate click product **P** would block the catalytic site of the nanorotor by a strong HETPHEN-type (HETeroleptic bis-PHENanthroline) complexation.[1b] Since product **P** possesses a zinc porphyrin (ZnPor) site, the binding

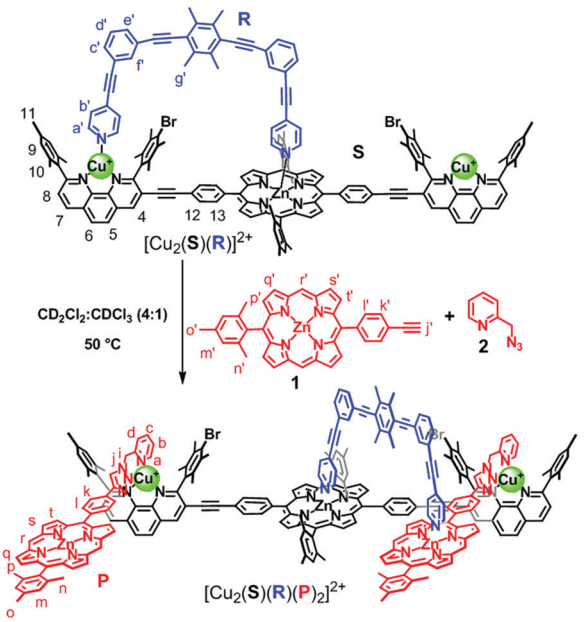

Scheme 1 Transformation of the nanorotor $[Cu_2(S)(R)]^{2+}$ to the slider-on-deck $[Cu_2(S)(R)(P)_2]^{2+}$.

Center of Micro and Nanochemistry and Engineering, Organische Chemie I, Universität Siegen, Adolf-Reichwein-Str. 2, Siegen D-57068, Germany.
E-mail: schmittel@chemie.uni-siegen.de; Tel: +49(0) 2717404356

† Electronic supplementary information (ESI) available: Experimental procedures, compound characterizations, spectral data, UV-vis titrations data. See DOI: 10.1039/d1cc02805g

‡ Abir Goswami and Merve S. Özer contributed equally.

of **P** should establish a new coordination site for the rotary biped in the nanorotor. With two ZnPor units coordinated to $[Cu_2(\mathbf{S})(\mathbf{R})]^{2+}$, another type of nanomechanical motion is expected in $[Cu_2(\mathbf{S})(\mathbf{R})(\mathbf{P})_2]^{2+}$ because it is formally a slider-on-deck system (Scheme 1), where the biped **R** should move between altogether three zinc porphyrins.[10c]

At first, we carried out a model catalytic study (Scheme 2) with the alkyne-terminated zinc(II) porphyrin **1** and 2-(azidomethyl)pyridine (**2**). They were allowed to react in a 1 : 1 ratio in CD_2Cl_2 : $CDCl_3$ (4 : 1) at 50 °C in the presence of an equimolar amount of $[Cu(\mathbf{Phen})]^+$, the copper(I)-loaded 2,9-dimesityl-1,10-phenanthroline. Progress of the reaction was followed by the signals of protons r-H and j′-H in the ^{1}H NMR (Fig. 1).

Disappearance of the signal of proton C≡CH (j′-H) and a single set of zinc porphyrin r-H, s-H, q-H, t-H and p-H signals in the ^{1}H NMR as well as the clean formation of $[Cu(\mathbf{Phen})(\mathbf{P})]^+$ indicated completion of the azide–alkyne cycloaddition reaction after ~24 h (ESI,† Fig. S19). Moreover, the signal of phenanthroline proton 2′-H experienced a diagnostic upfield shift from 7.01 to 6.74 ppm, showing that the copper(I)-loaded ligand was now coordinated to platform **P** (Fig. 1A and C). The emergence of a broad signal for the methylene protons i-H confirmed formation of the click product **P**. Finally, the single peak at m/z = 1205.3 in the ESI-MS proved the integrity of the heteroleptic complex $[Cu(\mathbf{Phen})(\mathbf{P})]^+$ (ESI,† Fig. S30).

After these exemplary catalytic investigations, we wanted to test the analogous click reaction with the rotor system as catalyst (Scheme 1). First of all, nanorotor $[Cu_2(\mathbf{S})(\mathbf{R})]^{2+}$ was prepared by mixing **S**, **R** and 2.0 equiv. of Cu^+ in CD_2Cl_2.[10a] The data unambiguously demonstrated that one pyridine foot of rotator **R** (= biped) was attached to the ZnPor unit of stator **S** by axial coordination while the other foot toggled between the Cu^+-loaded phenanthroline stations at a frequency k_{298} = 46.0 kHz. Activation parameters of the nanorotor $[Cu_2(\mathbf{S})(\mathbf{R})]^{2+}$ were reported earlier as $\Delta H^{\ddagger}$ = 49.1 ± 0.4 kJ mol^{-1} and $\Delta S^{\ddagger}$ = 9.5 ± 1.7 J mol^{-1} K^{-1}.[10a]

Finally, reactants **1** and **2** were heated with nanorotor $[Cu_2(\mathbf{S})(\mathbf{R})]^{2+}$ as a CuAAC[13] catalyst in a 2 : 2 : 1 ratio in CD_2Cl_2 : $CDCl_3$ (4 : 1) at 50 °C. Formation of $[Cu_2(\mathbf{S})(\mathbf{R})(\mathbf{P})_2]^{2+}$ was monitored by ^{1}H NMR spectroscopy and ESI-MS. Similar to the model reaction, the formation of platform **P** was followed by the disappearance of proton signals j′-H and *meso* r′-H of **1** and appearance of the *meso* r-H signal of **P** in ^{1}H NMR (Fig. 2C). Parallel, the peaks at m/z = 1970.8, 1606.0 and 1358.9 in the ESI-MS showed the expected mass signals for $[Cu_2(\mathbf{S})(\mathbf{R})(\mathbf{P})_2]^{2+}$, $[Cu_2(\mathbf{S})(\mathbf{R})(\mathbf{P})]^{2+}$ and $[Cu_2(\mathbf{S})(\mathbf{P})(CH_3CN)]^{2+}$, respectively

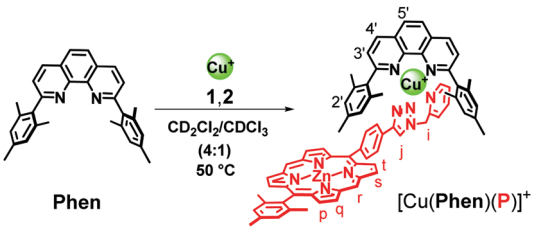

Scheme 2 Model study for self-sorting of platform **P** after formation with Click reaction.

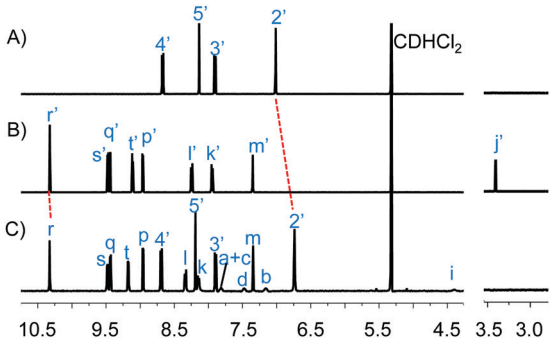

Fig. 1 Comparison of the partial ^{1}H NMR spectra (400 MHz, 298 K) in CD_2Cl_2 of (A) $[Cu(\mathbf{Phen})]^+$, (B) **1**, (C) $[Cu(\mathbf{Phen})(\mathbf{P})]^+$.

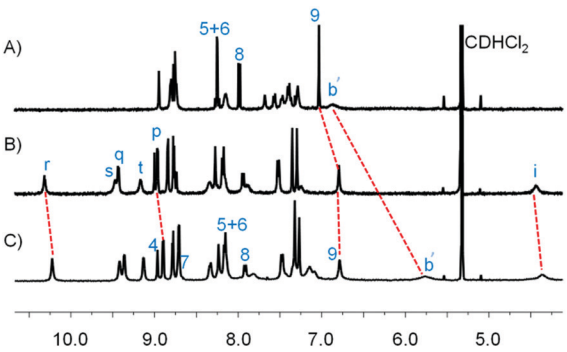

Fig. 2 Partial comparison ^{1}H NMR (400 MHz, 298 K) in CD_2Cl_2 of (A) nanorotor $[Cu_2(\mathbf{S})(\mathbf{R})]^{2+}$, (B) deck $[Cu_2(\mathbf{S})(\mathbf{P})_2]^{2+}$, (C) slider-on-deck $[Cu_2(\mathbf{S})(\mathbf{R})(\mathbf{P})_2]^{2+}$.

(ESI,† Fig. S32). The upfield shift of proton signal 9-H from 7.03 to 6.79 ppm indicated that platform **P** was coordinated to the Cu^+-loaded phenanthroline stations of stator **S** (Fig. 2A and C). Furthermore, the proton signal b′-H of rotator **R** shifted from 6.89 to 5.77 ppm as a result of the pyridine arm moving from the Cu^+-loaded phenanthroline station to the ZnPor platform. After 24 h, all the signals corresponding to **1** had disappeared and $[Cu_2(\mathbf{S})(\mathbf{R})(\mathbf{P})]^{2+}$ was furnished quantitatively.

To clearly establish the N_{py} → ZnPor coordination in slider-on-deck $[Cu_2(\mathbf{S})(\mathbf{R})(\mathbf{P})_2]^{2+}$, we separately prepared deck $[Cu_2(\mathbf{S})(\mathbf{P})_2]^{2+}$ by mixing **S**, **P** and $[Cu(CH_3CN)_4]PF_6$ in a 1 : 2 : 2 ratio in CD_2Cl_2 and compared it with $[Cu_2(\mathbf{S})(\mathbf{R})(\mathbf{P})_2]^{2+}$. In the ^{1}H NMR, the proton signal r-H resonating at 10.30 ppm experienced a notable upfield shift to 10.22 ppm when rotator **R** was added due to the axial pyridine coordination in slider-on-deck $[Cu_2(\mathbf{S})(\mathbf{R})(\mathbf{P})_2]^{2+}$. Furthermore, the DOSY spectrum yielded a single diffusion coefficient (D = 3.3 × 10^{-10} m^2 s^{-1}) indicating that the multi-component slider-on-deck $[Cu_2(\mathbf{S})(\mathbf{R})(\mathbf{P})_2]^{2+}$ was a single species. The experimental hydrodynamic radius was derived as 16.1 Å (ESI,† Fig. S17) in agreement with the theoretical value (ESI,† Fig. S34, S35). The system was further analyzed by UV-vis. In the final slider-on-deck, there are two different types of ZnPor units present; one emerging from stator **S** and two from both platforms **P**. The Q-band of **S** at 550 nm was reported earlier to undergo a red shift upon

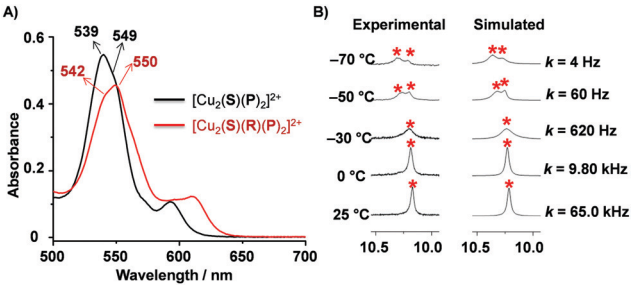

Fig. 3 (A) Comparison of the UV-vis spectra of $[Cu_2(\mathbf{S})(\mathbf{P})_2]^{2+}$ and $[Cu_2(\mathbf{S})(\mathbf{R})(\mathbf{P})_2]^{2+}$ in 1,1,2,2-tetrachloroethane (c = 1.00 mM, 298 K) in 1.0 mm cuvette. (B) Partial VT ^{1}H NMR (600 MHz) of slider-on-deck $[Cu_2(\mathbf{S})(\mathbf{R})(\mathbf{P})_2]^{2+}$ in CD_2Cl_2.

formation of rotor $[Cu_2(\mathbf{S})(\mathbf{R})]^{2+}$.[10a] In order to assign the ZnPor absorptions in $[Cu_2(\mathbf{S})(\mathbf{R})(\mathbf{P})_2]^{2+}$, the position of the ZnPor Q-band of **1** (536 nm) was determined in 1,1,2,2-tetrachloroethane (ESI,† Fig. S33). The Q-band absorption of the multicomponent deck $[Cu_2(\mathbf{S})(\mathbf{P})_2]^{2+}$ without rotator **R** (Fig. 3A) was observed at λ_{max} = 539 nm with a shoulder at 549 nm. The former absorption belongs to the ZnPor chromophore of **P** and the shoulder to the ZnPor unit of **S**. The Q-band absorption of the slider-on-deck system exhibited a λ_{max} = 550 nm with a hump at 542 nm (Fig. 3). As expected, upon coordination of **R** to the deck, the Q-bands experienced a red shift in agreement with our previous reports.[14]

After establishing the slider-on-deck system $[Cu_2(\mathbf{S})(\mathbf{R})(\mathbf{P})_2]^{2+}$, we examined the sliding motion of **R** across the three ZnPor units of deck $[Cu_2(\mathbf{S})(\mathbf{P})_2]^{2+}$ by VT (variable temperature) ^{1}H NMR (Fig. 3B and ESI,† Fig. S27, S28). The *meso* proton r-H (10.22 ppm) appearing as a singlet at 25 °C due to dynamic sliding showed coalescence at −30 °C and split at −50 °C into two singlets at a ratio of *ca.* 2 : 1. At −70 °C, splitting to 2 : 1 ratio can be seen more clearly. The signal at 10.28 ppm represents the N_{py} → ZnPor complexed site and the one at 10.22 ppm the pyridine-free ZnPor site. The software WinD-NMR[15] was used to simulate the VT ^{1}H NMR for the determination of the motion. The rate of exchange at room temperature was determined as k_{25} = 65.0 kHz and the corresponding activation parameters were calculated as $\Delta H^{\ddagger}$ = 49.4 ± 0.2 kJ mol^{-1} and $\Delta S^{\ddagger}$ = 13.1 ± 0.8 J mol^{-1} K^{-1} (Table 1). The kinetic barrier for exchange $\Delta G^{\ddagger}$ = 45.5 kJ mol^{-1} in $[Cu_2(\mathbf{S})(\mathbf{R})(\mathbf{P})_2]^{2+}$ is almost identical to that of a nanoslider that undoubtedly operates *via* a single N_{py} → ZnPor dissociation ($\Delta G^{\ddagger}$ = 47.3 kJ mol^{-1}).[14]

Finally, we coupled the slider-on-deck system with a base-catalyzed reaction (Scheme 3). From former work it had been established that the *N*-methylpyrrolidine (**5**) → ZnPor binding

Table 1 Experimental activation parameters of nanorotors and rotational frequency at 25 °C in CD_2Cl_2

Machines	$\Delta H^{\ddagger}$/kJ mol^{-1}	$\Delta S^{\ddagger}$/J mol^{-1} K^{-1}	$\Delta G^{\ddagger}$/kJ mol^{-1}	k_{298}/kHz
$[Cu_2(\mathbf{S})(\mathbf{R})]^{2+}$	49.1 ± 0.4[a]	9.5 ± 1.7[a]	46.6[a]	46.0[a]
$[Cu_2(\mathbf{S})(\mathbf{R})(\mathbf{P})_2]^{2+}$	49.4 ± 0.2	13.1 ± 0.8	45.5	65.0

[a] Ref. 10a

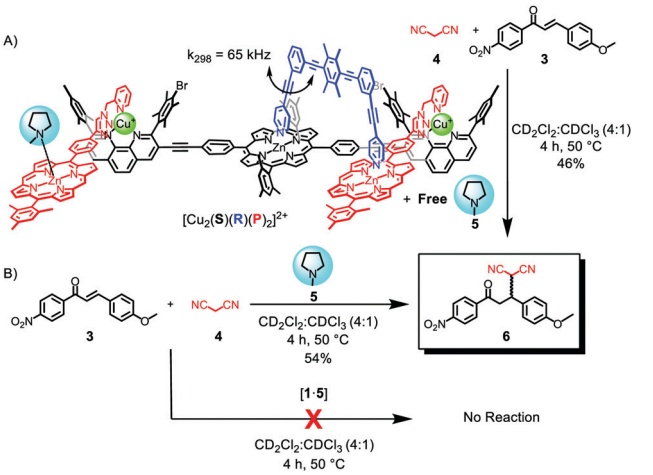

Scheme 3 (A) Catalyst liberation due to the sliding motion enables catalysis. (B) *N*-methylpyrrolidine (**5**) catalyzed Michael addition. Binding of **5** to ZnPor prevents catalysis.

was strong enough to prevent catalytic activity of the nitrogen heterocycle whereas sliding motion in slider-on-deck systems was found to liberate the bound catalyst (*N*-methylpyrrolidine → ZnPor-based sliders) into the solution thus turning ON catalysis.[10c] Hence, we expected that the catalyst *N*-methylpyrrolidine would be initially bound at the ZnPor unit of **1** thus being inactive for catalysis. However, after formation of the slider-on-deck $[Cu_2(\mathbf{S})(\mathbf{R})(\mathbf{P})_2]^{2+}$, the pyridyl end of the slider **R** would move from the Cu^+-loaded phenanthroline stations to the newly bound ZnPor platform and should liberate catalyst **5**. If this concept was correct, one would see that the *N*-methylpyrrolidine catalyzed reaction was turned ON.

To first check the ability of the slider-on-deck to act as a catalytic machinery in combination with organocatalyst **5**, we mixed **S** (1.9 mM), **P**, **R**, $[Cu(CH_3CN)_4]PF_6$, **3**, **4** and **5** in 1 : 2 : 1 : 2 : 20 : 100 : 2 ratio in CD_2Cl_2 : $CDCl_3$ (4 : 1) and heated at 50 °C. Indeed, 46% of the product **6** was formed after 4 h as evidenced by ^{1}H NMR (Scheme 3A). The reference reaction itself, the mixture of **3**, **4** and free catalyst **5** (3.8 mM) in 10 : 50 : 1 ratio in CD_2Cl_2 : $CDCl_3$ (4 : 1), furnished 54% of product **6** after heating at 50 °C for 4 h (Scheme 3B). This indicated that the dynamic slider-on-deck liberated most of the available catalyst **5** into solution as its activity is close to that of free **5**.

In the next step, the *in situ* evolution of the catalytic slider-on-deck and its effect on the Michael addition were tested. For that purpose, we mixed **1**, nanorotor $[Cu_2(\mathbf{S})(\mathbf{R})]^{2+}$ (≈ 2.0 mM) as well as **3**, **4** and catalyst **5** in 2 : 1 : 20 : 100 : 2 ratio in CD_2Cl_2 : $CDCl_3$ (4 : 1) and heated at 50 °C. No Michael addition product **6** was formed after 4 h because the static *N*-methylpyrrolidine (**5**) → ZnPor binding of **1** was strong enough to prevent catalytic activity (ESI,† Fig. S25).

To the same mixture, we added 2.0 equiv of azide **2** (with respect to the nanorotor) and heated at 50 °C. Now, 25% of the Michael addition product **6** formed after 4 h (ESI,† Fig. S24). The reduced yield of **6** may readily be rationalized by the fact that only 47% of the slider-on-deck was furnished after 4 h of heating. This yield agrees well with that of a control experiment

(44% of slider-on-deck formed in absence of the substrates after 4 h at 50 °C, see ESI,† Fig. S21), demonstrating that the formation of $[Cu_2(\mathbf{S})(\mathbf{R})(\mathbf{P})_2]^{2+}$ was itself not affected by the presence of compounds **3–5**. In summary, the findings show that catalyst **5** is liberated due to the formation of the slider-on-deck and as a result turns ON the Michael addition.

While supramolecular transformations are well established,[16] we demonstrate here how catalytic supramolecular machinery transforms itself into new catalytic machinery. In the key step a multicomponent machine catalyzes formation of an additional component that adds to its architecture.

In detail, the protocol involves the transformation of a nanorotor into a slider-on-deck system *via* copper(I)-catalyzed azide–alkyne cycloaddition (CuAAC).[13] While the motion of the nanorotor was dictated by the cleavage the coordinative $N_{py} \rightarrow [Cu(phenAr_2)]^+$ bond, after click reaction that of the slider-on-deck was guided by the $N_{py} \rightarrow$ ZnPor interaction. Consequently, the exchange speed changed, *i.e.* from 46.0 kHz (nanorotor) to 65.0 kHz (slider-on-deck). Moreover, the sliding motion was utilized to liberate a catalyst into the solution to turn ON a Michael addition. The formation of new catalytic machinery from a catalytically active nanorotor is a lucid example of an adaptive evolutionary process leading to new properties.

We are indebted to the Deutsche Forschungsgemeinschaft (Schm 647/20-2) for financial support and Dr. T. Paululat for VT NMR measurements.

Conflicts of interest

There are no conflicts to declare.

Notes and references

1 (*a*) J. M. Abendroth, O. S. Bushuyev, P. S. Weiss and C. J. Barrett, *ACS Nano*, 2015, **9**, 7746; (*b*) M. Schmittel, *Chem. Commun.*, 2015, **51**, 14956; (*c*) A. J. McConnell, C. S. Wood, P. P. Neelakandan and J. R. Nitschke, *Chem. Rev.*, 2015, **115**, 7729; (*d*) L. Zhang, V. Marcos and D. A. Leigh, *Proc. Natl. Acad. Sci. U. S. A.*, 2018, **115**, 9397; (*e*) A. Goswami, S. Saha, P. K. Biswas and M. Schmittel, *Chem. Rev.*, 2020, **120**, 125.
2 P. J. O'Brien and D. Herschlag, *Chem. Biol.*, 1999, **6**, R91.
3 Y. Yoshikuni, T. Ferrin and J. Keasling, *Nature*, 2006, **440**, 1078.
4 (*a*) J.-M. Lehn, *Angew. Chem., Int. Ed.*, 2013, **52**, 2836; (*b*) A. Goswami, T. Paululat and M. Schmittel, *J. Am. Chem. Soc.*, 2019, **141**, 15656; (*c*) J. Andréasson and U. Pischel, *Coord. Chem. Rev.*, 2021, **429**, 213695; (*d*) F. Nicoli, E. Paltrinieri, M. Tranfić Bakić, M. Baroncini, S. Silvi and A. Credi, *Coord. Chem. Rev.*, 2021, **428**, 213589.
5 (*a*) S. Silvi, A. Arduini, A. Pochini, A. Secchi, M. Tomasulo, F. M. Raymo, M. Baroncini and A. Credi, *J. Am. Chem. Soc.*, 2007, **129**, 13378; (*b*) S. Hiraoka, Y. Hisanaga, M. Shiro and M. Shionoya, *Angew. Chem., Int. Ed.*, 2010, **49**, 1669; (*c*) Y. Takara, T. Kusamoto, T. Masui, M. Nishikawa, S. Kume and H. Nishihara, *Chem. Commun.*, 2015, **51**, 2896.
6 (*a*) R. Herges, *Chem. Sci.*, 2020, **11**, 9048–9055; (*b*) S. Corra, M. Curcio, M. Baroncini, S. Silvi and A. Credi, *Adv. Mater.*, 2020, **32**, e1906064; (*c*) A. W. Heard and S. M. Goldup, *ACS Cent. Sci.*, 2020, **6**, 117; (*d*) S. Krause and B. L. Feringa, *Nat. Chem. Rev.*, 2020, **4**, 550; (*e*) J. Echavarren, M. A. Y. Gall, A. Haertsch, D. A. Leigh, J. T. J. Spence, D. J. Tetlow and C. Tian, *J. Am. Chem. Soc.*, 2021, **143**, 5158; (*f*) Y. Feng, M. Ovalle, J. S. W. Seale, C. K. Lee, D. J. Kim, R. D. Astumian and J. F. Stoddart, *J. Am. Chem. Soc.*, 2021, **143**, 5569.
7 G. de Bo, M. A. Y. Gall, S. Kuschel, J. de Winter, P. Gerbaux and D. A. Leigh, *Nat. Nanotechnol.*, 2018, **13**, 381.
8 (*a*) J.-M. Lehn, *Angew. Chem., Int. Ed.*, 2013, **52**, 2836; (*b*) R. Merindol and A. Walther, *Chem. Soc. Rev.*, 2017, **46**, 5588.
9 M. Raynal, P. Ballester, A. Vidal-Ferran and P. W. N. M. van Leeuwen, *Chem. Soc. Rev.*, 2014, **43**, 1734.
10 (*a*) A. Goswami, S. Pramanik and M. Schmittel, *Chem. Commun.*, 2018, **54**, 3955; (*b*) N. Mittal, M. S. Özer and M. Schmittel, *Inorg. Chem.*, 2018, **57**, 3579; (*c*) I. Paul, A. Goswami, N. Mittal and M. Schmittel, *Angew. Chem., Int. Ed.*, 2018, **57**, 354; (*d*) A. Goswami and M. Schmittel, *Angew. Chem., Int. Ed.*, 2020, **59**, 12362.
11 Z. He, W. Jiang and C. A. Schalley, *Chem. Soc. Rev.*, 2015, **44**, 779.
12 P. K. Biswas, S. Saha, T. Paululat and M. Schmittel, *J. Am. Chem. Soc.*, 2018, **140**, 9038.
13 (*a*) M. Meldal and C. W. Tornøe, *Chem. Rev.*, 2008, **108**, 2952; (*b*) M. Meldal and F. Diness, *Trends Chem.*, 2020, **2**, 569.
14 A. Goswami, I. Paul and M. Schmittel, *Chem. Commun.*, 2017, **53**, 5168.
15 H. J. Reich, *NMR Spectrum Calculations: WinDNMR, Version 7.1*, Department of Chemistry, University of Wisconsin.
16 (*a*) W. Wang, Y.-X. Wang and H.-B. Yang, *Chem. Soc. Rev.*, 2016, **45**, 2656; (*b*) W. M. Bloch, J. J. Holstein, W. Hiller and G. H. Clever, *Angew. Chem., Int. Ed.*, 2017, **56**, 8285; (*c*) G. Li, Z. Zhou, C. Yuan, Z. Guo, Y. Liu, D. Zhao, K. Liu, J. Zhao, H. Tan and X. Yan, *Angew. Chem., Int. Ed.*, 2020, **59**, 10013.